Catalytic synthesis of 2-methyl pyrazine over Zn-modified zeolites

R. Anand, S.G. Hegde, B.S. Rao, and Chinnakonda S. Gopinath *

Catalysis Division, National Chemical Laboratory, Dr. Homi Bhabha Road, Pune 411 008, India

Received 5 July 2002; accepted 14 September 2002

Cyclization of ethylene diamine and propylene glycol to 2-methyl pyrazine (2-MP) was investigated on Zn-modified zeolites, namely ZSM-5, Beta, and ferrierite catalysts, as a function of temperature, space velocity, and feed ratio. Zn-impregnated ZSM-5 was found to be the promising catalyst with 64% selectivity for 2-MP at 450 °C. ZnO-like species on Zn-impregnated ZSM-5, identified from XPS, enhance the selectivity to 2-MP. The difference in acidity, the nature of the Zn species, and its distribution on Zn-modified ZSM-5 catalysts obtained from FT-IR and XPS are in good agreement and they are correlated with catalytic activity.

KEY WORDS: methyl pyrazine; zeolite; zinc oxide; ZSM-5; alkyl pyrazines; XPS; FT-IR.

1. Introduction

Pyrazine and alkylpyrazines are used in flavors, fragrances, and pharmaceutical intermediates. Among them, 2-methylpyrazine (2-MP) is used as a raw material of the anti-tuberculosis drug pyrazinamide [1]. Currently, they are prepared by dehydration–cyclization and/or partial dehydrogenation of ethylene diamine (ED) and propylene glycol (PG) [2]. Catalytic systems based on Cu–Cr [3], Cu–Zn–Cr [4], zinc–phosphoric acid–manganese [5], and Ag [6] are patented for preparation of 2-MP from ED and PG. Forni *et al.* extensively studied this reaction over palladized zinc–chromium oxide [7] and Pd-promoted ZnO–$ZnCr_2O_4$ mixture [8]. Other studies include $MnSO_4$–H_3PO_4–ZnO [9], Ag–La/Al_2O_3 [10], ZnO–WO_3 mixture [11], and modified ZSM-5 and chromite catalysts [12]. However, the synthesis of 2-MP was not well studied over acidic zeolites (both medium and large pore) due to the complexity involved in such cyclization reactions and cracking of the substrates over acidic zeolites. Recently we reported the synthesis of 2-MP over zinc-modified ferrierite (FER) [13]. It is also reported that zinc-modified MFI-type zeolites are important catalysts for conversion of paraffins [14–17], and it is also known that ZnO catalyzes effectively in both dehydration and dehydrogenation reactions [18]. For the present studies, H-ZSM-5 and Zn-modified zeolite catalysts (ZSM-5, FER, and Beta) were selected for this reaction. ZnO-impregnated ZSM-5 shows comparable or better catalytic activity compared to earlier catalysts [3–12].

* To whom correspondence should be addressed.
E-mail: gopi@cata.ncl.res.in

2. Experimental

2.1. Catalyst synthesis and characterization

ZSM-5 [19] and FER [20] zeolite catalysts were synthesized as reported in the literature. The zeolite Beta was procured from P.Q. Corporation, The Netherlands. The ZnO-impregnated zeolites (ZnO-zeolite) were prepared by mixing hydrogen forms of respective zeolites (10 g) with zinc acetate (1.35 g) in distilled water (100 ml). The mixture was digested at 80 °C for 5 h, dried and calcined at 550 °C. Ion exchange of ZSM-5 zeolite was carried out at 90 °C using 0.5 M zinc acetate solution for 16 h. The ion-exchanged ZSM-5 zeolite (Zn-ZSM-5) was washed with de-ionized water, dried at 110 °C, and calcined at 550 °C for 12 h. The crystallinity and phase purity of zeolites were confirmed by XRD (Rigaku, D-Max III VC diffractometer with Cu K_α radiation of $\lambda = 1.5404$ Å). The chemical compositions of zeolites were determined by a wavelength dispersive X-ray fluorescence (3070 Rigaku) spectrophotometer. Energy dispersive X-ray (EDX) analysis was employed to determine the amount of zinc oxide impregnated. An Omnisorp 100 CX (Coulter Corporation, USA) analyzer was used for surface area measurement.

X-ray photoelectron spectra (XPS) were recorded in the Vacuum Generator's Microtech Multilab ESCA 3000 spectrometer with an Mg K_α X-ray source in a vacuum of $1–3 \times 10^{-9}$ torr range during the analysis. Energy resolution of the instrument is set to 0.8 eV at a pass energy of 20 eV [21]. Accuracy of the binding energy (BE) reported is within ±0.1 eV. Photoionization cross section (σ) [22] was used to obtain compositions of the surface and atom ratios from peak areas.

1011-372X/02/1200-0265/0

2.2. Acidity measurement by TPD and FT-IR

2.2.1. TPD-NH_3

An Autochem 2910 instrument (Micromeritics) was employed for the temperature-programmed desorption of ammonia (TPD-NH_3) in order to determine the distribution of acid sites on the catalysts. The desorption process was monitored by a TCD detector. 400 mg of the calcined catalyst were used for each experiment. Prior to analysis, the catalyst was pretreated *in situ* for 2 h in an He flow (30 ml/min) at 450 °C. NH_3 adsorption was performed by passing NH_3 in an He stream over the catalyst for 30 min at 50 °C. The physisorbed NH_3 was removed by holding the sample at the adsorption temperature for 1 h in the He flow of 50 ml/min. TPD profiles of NH_3 were obtained from 50 to 700 °C at a heating rate of 10 °C/min.

2.2.2. FT-IR spectroscopy

Pyridine adsorption–desorption was monitored by FT-IR spectroscopy. Self-supported wafers of zeolite samples (15–20 mg/cm^2) were evacuated *in situ* (400 °C, 3 h, 10 Pa) in a Pyrex cell with KBr windows. Catalysts were treated with pyridine at 100 °C and subsequently desorbed at increasing temperature (100–400 °C) in dynamic vacuum. The spectra were recorded using a Nicolet 60 SXB spectrometer with a resolution of 2 cm^{-1} averaging over 500 scans. Brønsted and Lewis acid sites were determined from the area of the adsorbate PyB band near 1540 cm^{-1} and the PyL band near 1450 cm^{-1} [23], respectively.

2.3. Catalytic reactions and product analysis

The catalytic activity measurements were carried out at atmospheric pressure in a fixed-bed down-flow integral reactor using 3 g of the catalyst (10–20 mesh sizes) at temperatures between 300 and 450 °C. The catalyst was activated in a flow of dry air at 500 °C for 5 h prior to catalytic runs. The catalyst was then flushed with dry N_2 and cooled to reaction temperature. The reactant feed was prepared by mixing ED, PG, and water in the mole ratio of 1 : 1 : 5 and the liquid reactants were fed into the reactor by a syringe feed pump (SAGE instruments, model 352, USA) at the required rate. Water helped in reducing the viscosity and smooth feeding of the reactants. The liquid products were analyzed by GC (15A, Shimadzu) using an OV-101 column and confirmed by GC-MS (QP 200A, Shimadzu) and GC-FT-IR (Perkin Elmer, FT-IR spectrometer 2000). The mass balance was >90%. In the absence of water, high coking was observed.

3. Results and discussion

3.1. Catalyst characterization

Physico-chemical characteristics of Zn-modified zeolites are shown in table 1. An XRD pattern indicates that the zeolite samples used are highly crystalline (results not shown). The Zn-modification of the parent zeolite did not affect the crystal structure of the zeolites, and XRD patterns for the modified zeolites were the same as that of the parent zeolite. The three ZnO-modified catalysts contain ZnO around 4.5% by weight.

TPD-NH_3 profiles of virgin, Zn-modified, and H-ZSM-5 samples are shown in figure 1. The Si/Al ratio of ZSM-5 used for modification with zinc was 100. The virgin sample displays two desorption peaks each in the low-temperature (LT, $T < 300$ °C) and high-temperature region (HT, $T > 300$ °C). The second peak in the LT region may be due to the possible formation of $NH_4^+ \cdot nNH_3$ associations [24,25]. The TPD-NH_3 results for zinc-modified ZSM-5 zeolites are also shown in table 1. Figure 1 reveals for Zn-modified ZSM-5 an overall widening of the desorption profile with new peaks, and HT peaks shift to higher temperatures compared to virgin ZSM-5. This clearly indicates the generation of new adsorption sites. The HT of Zn-modified ZSM-5 shows a shoulder and the LT peak is widened and shifted to high temperature. These changes could be attributed to the generation of strongly acidic Lewis

Table 1
Physico-chemical characteristics of ZnO-modified zeolites.

Catalyst	H-ZSM-5	ZnO-ZSM-5	Zn-ZSM-5 (exchanged)	ZnO-FER	ZnO-Beta
Si/Al ratio	100.0	100.0	100.0	17.0	15.0
Zn content (wt%) [a]	0.0	4.52	2.11	4.6	4.5
Surface area (m^2/g)	372.6	314.7	322.6	214.4	404.9
TPD-T_{d1} [b]	0.12	0.12	0.11	0.35	0.38
TPD-T_{d2} [b]	0.15	0.45	0.32	0.06	1.62
Brønsted : Lewis acid ratio [c]	2.97	0.31	0.09	–	–

[a] Zinc weight percentage calculated from XRF and EDX.
[b] $T_{d1} < 300$ °C; $T_{d2} > 300$ °C.
[c] Calculated from FT-IR spectra of adsorbed pyridine.

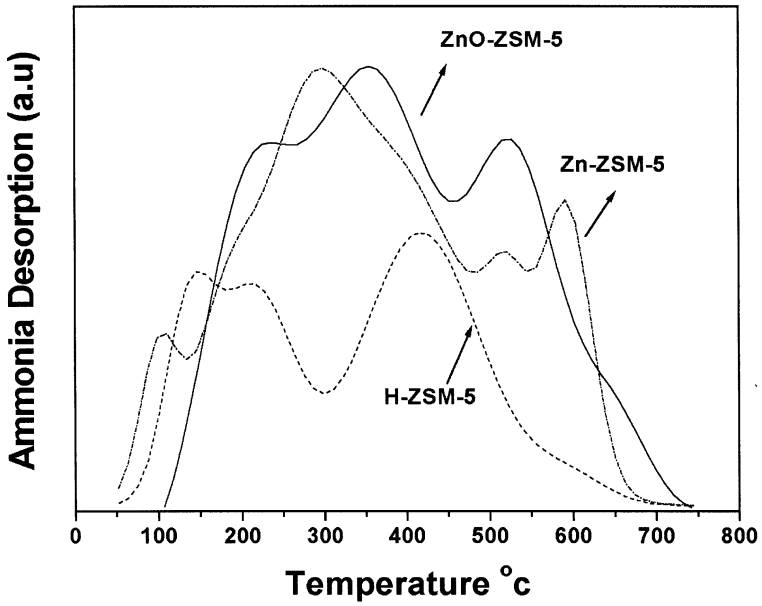

Figure 1. NH_3-TPD spectra of H-ZSM-5 and zinc-modified H-ZSM-5 samples.

sites. Both ZnO-ZSM-5 and Zn-ZSM-5 zeolites show a distinct increase of NH_3 desorption by 0.30 and 0.17 mmol/g, respectively, compared to H-ZSM-5. Total acidity of the samples decreases in the following order: ZnO-ZSM-5 > Zn-ZSM-5 > H-ZSM-5. Osaka *et al.* [26] have reported a shift of the LT peak indicating an interaction of Zn with NH_3. Roessner *et al.* [27] also relate the increase of LT peak to the formation of Lewis sites generated by Zn^{2+}, and an additional tailing of the HT peak is due to strongly acidic Lewis sites. Biscardi and Iglesia [28] showed that ion exchange leads to intrazeolitic zinc centers, while impregnation leads to exchanged centers and extracrystalline ZnO.

In figure 2, FT-IR spectra of structural hydroxy groups of Zn-modified and virgin H-ZSM-5 are given. Relatively a high background observed is to be noted on ZnO-ZSM-5. All three samples show peaks due to three different OH groups at almost the same frequencies (denoted by arrows); only the Zn-exchanged sample shows an additional peak around 3635 cm^{-1}. A remarkable difference can be noticed in the relative concentration of different kind of OH groups. Despite the high Zn^{2+} (4.5%) concentration on ZnO-ZSM-5, high-frequency OH groups are comparatively less in intensity than on virgin and Zn-exchanged ZSM-5 samples. It is evident from figure 2 that the concentration of the surface silanol groups at 3740 cm^{-1} and bridging OH groups (Si–OH–Al at 3650 cm^{-1}) in the impregnated sample has decreased considerably more than in the ion-exchanged sample. This indicates that in the impregnated sample, in addition to ion-exchangeable positions, zinc may be present as bulk ZnO on the surface. Difference IR spectra of the pyridine region (1700–1400 cm^{-1}) of all ZSM-5 catalysts at 200 °C after pyridine adsorption and activated surface at 100 °C (before pyridine adsorption) are shown in figure 3, and the ratio of Brønsted to Lewis acid sites is shown in table 1. It is clear from figure 3 and table 1 that the number of Lewis acid sites is almost the same and is high in Zn-modified catalysts; however, the number of Brønsted acid sites is low on Zn-ZSM-5 catalyst, indicating that all the exchangeable sites are occupied with Zn. That Zn-impregnation also leads to Zn-exchange to a good extent is evident from the decrease in Brønsted acid sites.

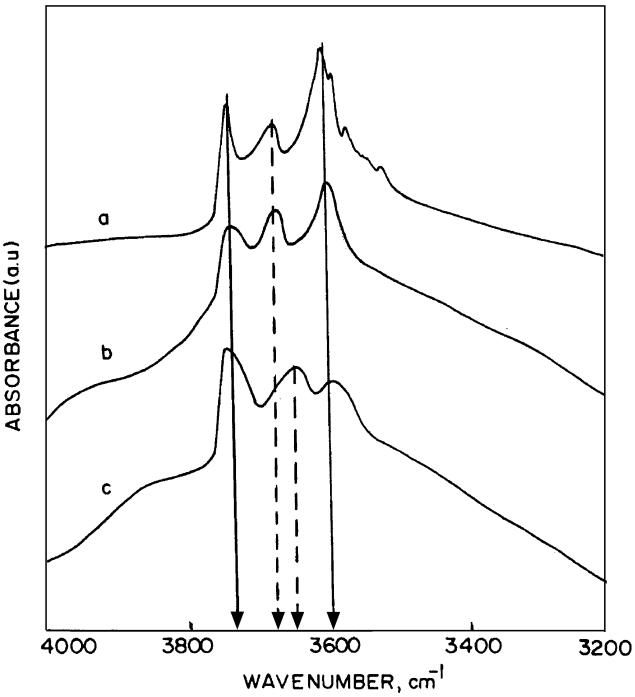

Figure 2. FT-IR spectra in structural hydroxyl group vibrations: (a) H-ZSM-5, (b) ZnO-ZSM-5, and (c) Zn-ZSM-5.

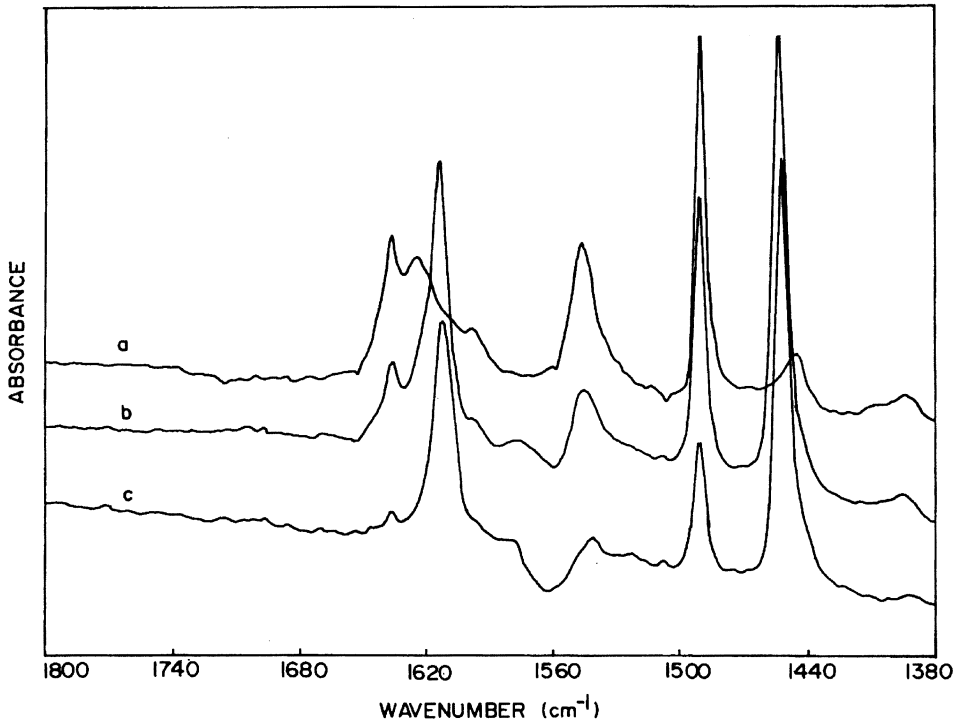

Figure 3. FT-IR difference spectra of pyridine adsorbed at 200 °C on (a) H-ZSM-5, (b) ZnO-ZSM-5, and (c) Zn-ZSM-5.

XPS studies were carried out on Zn-modified ZSM-5 catalysts to understand the nature and distribution of zinc species. Figure 4 shows the Zn $2p_{3/2}$ core-level spectrum from impregnated ZnO-ZSM-5, Zn-ZSM-5, a physical mixture of ZnO (5%) and ZSM-5 and pure ZnO. Further, the Zn $2p_{3/2}$ spectra from the impregnated and ion-exchanged zeolites are deconvoluted (figures 4(b) and (c)). XPS parameters derived from all the above catalysts are given along with Si 2p BE in table 2. It is clear from figure 4(a) that the BE of the Zn $2p_{3/2}$ core level from all the above catalysts is comparable to ZnO and in good agreement with the results reported earlier [29]. This clearly indicates that the nature of Zn species is close to that of ZnO. However, there is a broadening associated with all catalysts, indicating that there might be more than one species, and the deconvolution indeed shows that there are two different Zn species at different BE. Species 2 appears at 1023.3 eV in impregnated as well as in ion-exchanged cases, and is similar to that of ZnO and large in quantity. However, species 1 appears at lower BE than that of ZnO and is low in intensity. It is speculated here that species 1 could be from the Zn species that are incorporated into the zeolite lattice.

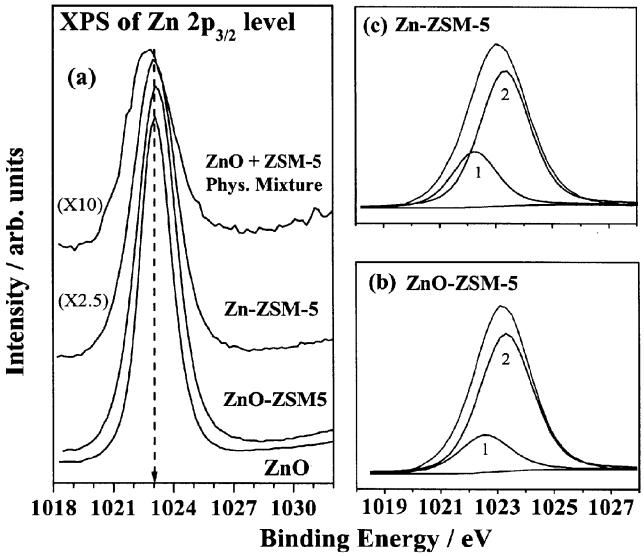

Figure 4. (a) Zn $2p_{3/2}$ core-level spectrum from ZnO, ion-exchanged ZSM-5 (Zn Exc. ZSM-5), impregnated ZSM-5 (ZnO-ZSM-5) and a physical mixture of ZnO (5%) and ZSM-5. Note that the spectra from the exchanged and the physical mixture are multiplied by factors shown in the figure to have comparable intensity with that of impregnated zeolite. The impregnated and exchanged zeolite Zn $2p_{3/2}$ spectra are deconvoluted in (b) and (c), respectively.

Table 2 demonstrates that the surface Zn/Si ratio is low for Zn-ZSM-5 compared to impregnated ZnO-ZSM-5. In the case of physical mixture it is too low. The values obtained for the surface Zn/Si ratio suggest that the distribution of Zn species is more uniform and well separated on both Zn-modified ZSM-5 catalyst surfaces. The Zn/Si ratio is double on impregnated compared to ion-exchanged samples, indicating higher Zn concentration on the surface. However, the physical mixture shows very poor Zn concentration on the surface. The low intensity of silanol groups from IR (figure 2) and relatively high Zn/Si ratio from XPS on Zn-impregnated samples (figure 4 and table 2) are in good agreement.

Table 2
XPS parameters of different zinc ZSM-5 catalysts and ZnO.

Material	Zn $2p_{3/2}$ (FWHM) (eV)		Si 2p (eV)	$(Zn/Si)_{XPS}$	
	Species 1	Species 2		Species 1	Species 2
ZnO	–	1023.1 (1.9)	–	–	–
ZnO-ZSM5	1022.6 (2.1)	1023.3 (2.2)	103.3	0.0724	0.263
Zn-ZSM-5	1022.3 (1.9)	1023.3 (2.1)	103.4	0.05	0.131
Physical mixture (ZnO (5%) and ZSM-5)	1022.8 (2.6)	1022.8 (2.6)	103.8	0.027	0.027

3.2. Catalytic reaction products

The reaction generally occurs through a dehydrocyclization route at acidic centers. It is reported by Kulkarni *et al.* [12] that the interstitial Brønsted acid centers are particularly responsible for the conversion of PG and ED to the N-containing heterocycles through intermolecular and intramolecular cyclization. ED and PG combine to give 2-methyl piperazine, the intermediate product, which dehydrogenates to form 2-MP. Other compounds formed are alkyl pyrazines with alkyl groups like dimethyl, ethyl, methylethyl, and propyl. Pyrazine is also formed by the dealkylation of alkyl pyrazines. Low boilers observed are CO_2, CH_3CHO, ethanol, acetone, propionaldehyde, 2-propen-1-ol, *n*-propanol, and 2-butanone.

Feeding pure PG over ZnO-modified zeolites results in the formation of acetone and aromatics like benzene, toluene, and xylenes (BTX) with less percentage of the low boilers. Piperazine, pyrazine, and alkylpyrazines were the products of the self-reaction of ED over these Zn-modified zeolites. With both ED and PG in the feed, BTX were not found, indicating that intermolecular cyclization is the main reaction. The cracked products of ED and/or PG interact with piperazines and pyrazines to form other alkylpyrazines. The amount of these products is less compared to that obtained during the cyclization reaction.

3.3. Temperature dependence

The effect of temperature on the conversion and product selectivity in the case of ZnO-ZSM-5 for 2 h time on stream at a WHSV of $1\,h^{-1}$ is presented in figure 5(a). The PG conversion increased from 55% at 300 °C to 100% at 400 °C. Considerable amounts of low boilers (11–34%) were detected. At low temperatures these were considerable, and at high temperatures—even though they are expected to be high, due to the reaction of some of these compounds, like methanol and acetaldehyde, with piperazine and pyrazine, giving alkyl pyrazines—a reduction in their concentration is observed. It is reported that piperazine or its alkyl derivatives were dehydrogenated easily to the corresponding pyrazine derivative over ZnO-modified catalyst. Formation of ethyl pyrazine, dimethyl pyrazine, ethylmethyl pyrazine and propyl pyrazine were observed with all the catalysts studied. The product pattern for ZnO-FER (figure 5(b)) is similar to that obtained for ZnO-ZSM-5 zeolite. However, the selectivity of 2-MP was low at 300 °C (7.1%) and increased sharply to 38% at 400 °C. In this case, formation of a large amount of low boilers was noted at low temperatures (63%). Since the conversion of PG is less at low temperatures, the formation of pyrazines and piperazines was much less compared to that of other catalyst systems under study. ZnO-Beta shows a selectivity of 30% for methyl piperazine at 300 °C (figure 5(c)) and the same decreases to 1.8% at 400 °C. ZnO-Beta afforded a large amount of 2-methyl-piperazine and pyrazine showing high activity towards the cyclization reaction, compared to the other two catalysts.

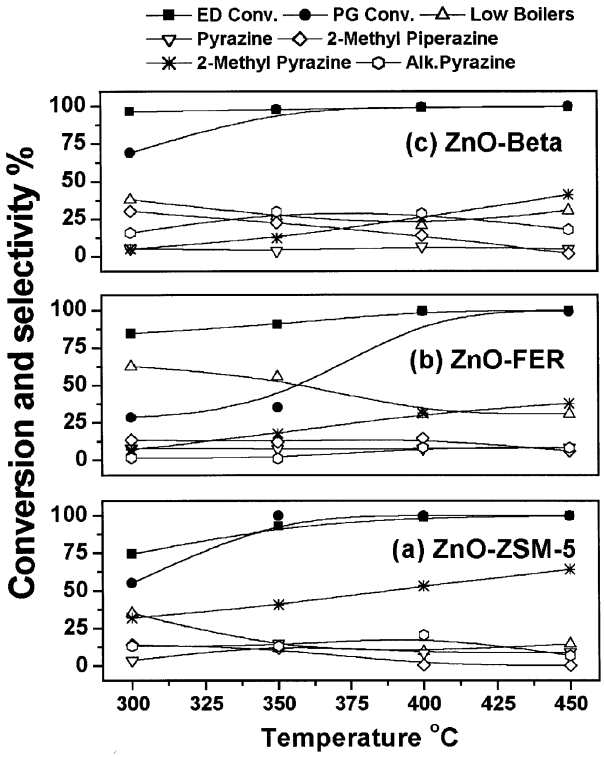

Figure 5. Effect of temperature on synthesis of 2-MP over ZnO-modified zeolites. Reaction conditions are: atmospheric pressure, WHSV = $1\,h^{-1}$, time on stream = 2 h, and ED : PG : water (1 : 1 : 5) mole ratio.

3.4. Effect of time on stream

An investigation of the conversion and the product selectivity as a function of time at 400 °C over the ZnO-ZSM-5 zeolite reveals (figure 6(a)) that the conversion of ED decreases from 99 to 97% after 8 h of reaction. It is to be noted that the percentage conversion ratio of ED : PG of 1 : 1 hints that the primary reaction is intermolecular cyclization. Nonetheless, 2-MP concentration gradually decreased from 53 to 37% with a slight increase in the selectivity for low boilers. This trend is observed for all the zeolites studied. These results indicated that all catalysts display stable activity in the conversion of ED and PG but not to the desired products due to secondary reactions. The deactivation is comparably faster in the case of ZnO-FER (figure 6(b)); the conversion of ED dropped sharply from 99 to 90% after 3 h and showed a constant conversion up to 7 h. The selectivity of the 2-MP decreased and that of 2-methylpiperazine increased with time on stream, showing that dehydrogenation has not taken place. ZnO-Beta (figure 6(c)), which is not selective for 2-MP as compared to ZnO-ZSM-5, afforded a lot of dimethyl pyrazines, ethyl pyrazines, ethylmethyl pyrazines and propyl pyrazines with a concomitant increase in the formation of pyrazine, which may be due to the structural differences between Beta and the other zeolites.

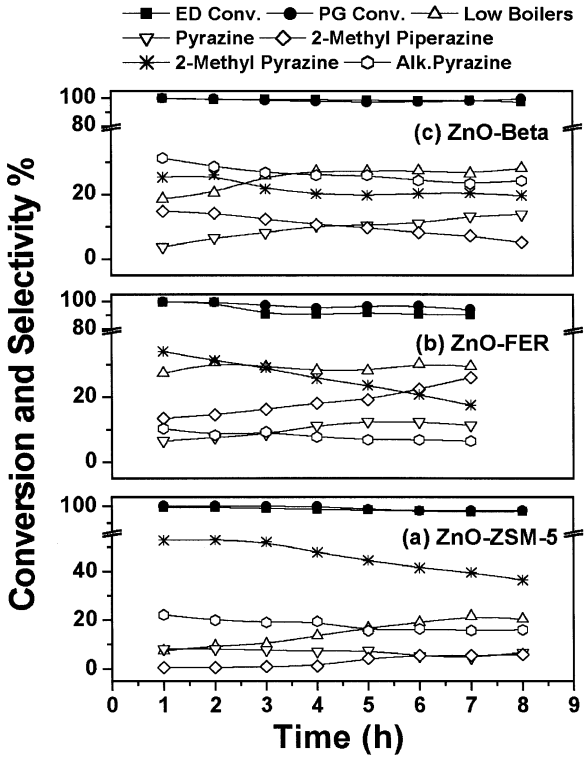

Figure 6. Effect of time on stream on the selectivity of 2-MP over ZnO-modified zeolites. Reaction conditions are: atmospheric pressure, temperature = 400 °C, WHSV = 1 h^{-1}, and ED : PG : water (1 : 1 : 5) mole ratio.

3.5. Dependence on weight hourly space velocity

Figure 7 displays the effect of weight hourly space velocity (WHSV) on the conversion and product selectivity at 400 °C on (a) ZnO-ZSM-5, (b) ZnO-FER and (c) ZnO-Beta. In general, with all three catalysts, conversion remains very high; nonetheless the selectivity towards 2-MP decreases and that for 2-methylpiperazine increases with WHSV, indicating the lack of dehydrogenation at low contact time. The formation of 2-MP and the other alkyl pyrazines was greater at low WHSV. For example, on ZnO-ZSM-5, more methyl piperazine was observed at higher WHSV (2 h^{-1}), whereas at low WHSV it undergoes dehydrogenation and leads mostly to pyrazines. A similar product pattern is observed on the other two catalysts at different levels. The formation of a large amount of low boilers and some unidentifiable high boilers at higher WHSVs is also worth noting. The percentage selectivity values lead to the conclusion that the dehydrogenation activity of ZnO-FER and ZnO-Beta is less than that of ZnO-ZSM-5 and hence there is considerable selectivity of 2-MP even at high WHSV on ZnO-ZSM-5.

3.6 Effect of molar ratio of reactants

In order to find out the optimum feed ratio, a series of experiments were performed at 400 °C with different mole ratios of ED and PG over ZnO-ZSM-5, and the results are given in table 3. Molar ratio was found to

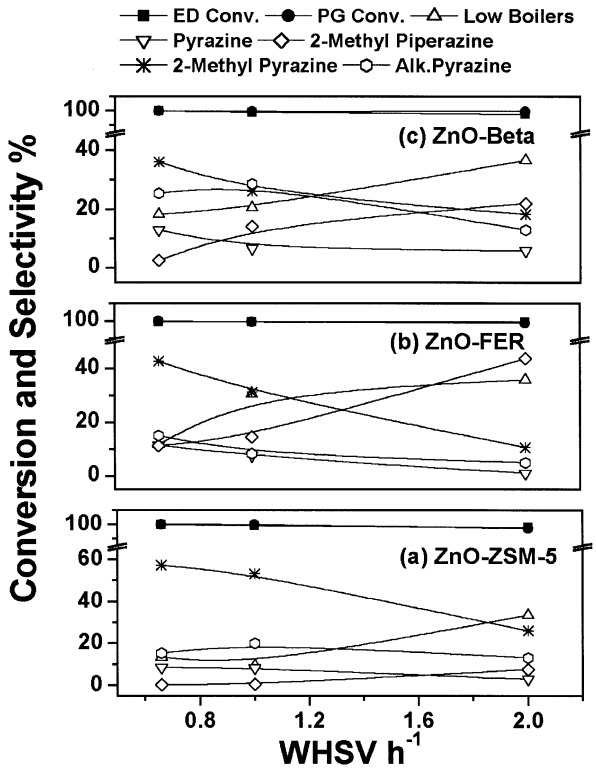

Figure 7. Effect of WHSV on the selectivity of 2-MP over ZnO-modified zeolites. Reaction conditions are: atmospheric pressure, temperature = 400 °C, time on stream = 2 h, and ED : PG : water (1 : 1 : 5) mole ratio.

Table 3
Effect of molar ratio of ethylene diamine and propylene glycol on synthesis of 2-methyl pyrazine over ZnO-ZSM-5.

Molar ratio (ED : PG)	ED conv.	PG conv.	LB	PY	MPIP	2-MP	Alk. pyrazine	Others
1 : 2	99.2	95.0	25.4	3.9	1.0	45.0	11.6	13.1
1 : 1.5	99.4	99.0	15.4	6.0	0.8	48.5	19.5	9.8
1 : 1	99.1	100.0	9.4	8.2	0.5	53.1	20.3	8.5
1.5 : 1	97.5	97.7	9.5	9.0	3.2	59.5	15.0	3.8
2 : 1	96.2	98.1	10.9	11.6	3.3	63.5	7.7	3.0

ED = ethylene diamine; PG = propylene glycol; LB = low boilers; PY = pyrazine; MPIP = methyl piperazine; 2-MP = 2-methyl pyrazine. Reaction conditions: atmospheric pressure, temperature = 400 °C; WHSV = 1 h^{-1}; TOS = 2 h; ED : PG : water = 1 : 1 : 5 mole ratio.

have a profound effect over the reaction. Production of 2-MP increases with an increase in ED concentration in the feed. This is due to the self-cyclocondensation of ED leading to pyrazine and alkylpyrazine, which was noted while feeding ED alone. It can also be noted that the formation of methylpiperazine, a primary product, was found in a noticeable amount in the feed when ED concentration was higher.

3.7. Effect of zinc modification

The catalytic activity results of various Zn-modified catalysts are shown in table 4. It is observed that the conversion of both ED and PG over ZnO is less as compared with the ZnO zeolites. However, ZnO produced a somewhat higher selectivity for 2-MP as compared to ZnO zeolites even though a higher amount of low boiling compounds are formed. Virgin H-ZSM-5 showed very low selectivity to 2-MP and produced a higher amount of side products (alkylpyrazines and high boilers). A physical mixture of ZnO and H-ZSM-5 also produced a similar result. Both zinc-modified ZSM-5 (ion-exchange and impregnated) samples show a better catalytic activity than the above three catalysts, ZnO-FER and ZnO-Beta. The better activity associated with Zn-modified catalysts is attributed mainly to two factors, namely, large numbers of Lewis acid sites and a relatively large amount of Zn and its optimum distribution on the surface. IR studies demonstrated that both Zn-ZSM-5 and ZnO-ZSM-5 catalysts show similar amounts of Lewis acid sites, but more Zn is evident on the ZnO-ZSM-5 than the Zn-ZSM-5 catalyst from XPS studies. Further, the extracrystalline ZnO observed from XPS and FT-IR studies on the ZnO-ZSM-5 sample might enhance the catalytic activity.

4. Conclusions

Reaction of ED and PG over ZnO-modified zeolites, in general, resulted in the formation of methyl pyrazine. Zn-ZSM-5 catalyst shows considerable catalytic activity due to large amounts of Lewis acid sites. ZnO-ZSM-5 displayed higher selectivity towards 2-MP than any other zinc-modified zeolites in the present study and this is attributed to the high Lewis acid character in combination with large amounts of Zn distributed optimally on the surface. Crystalline ZnO observed on the ZnO-ZSM-5 catalyst also might enhance the activity. ZnO-Beta and ZnO-FER are less active and ZnO-Beta is not selective. Higher amounts of ED in the feed improve the selectivity of 2-MP. The stability of these catalysts in terms of conversion of ED with time on stream followed the order ZnO-ZSM-5 > ZnO-Beta > ZnO-FER. Low contact time prevents the dehydrogenation step of piperazine to pyrazines to a large extent.

Acknowledgments

We thank Dr. K.V.R. Chary, IICT, Hyderabad, for help in recording the TPD data. R.A. thanks CSIR, New Delhi, India, for a senior research fellowship.

Table 4
Effect of various catalysts on synthesis of 2-methyl pyrazine.

Catalyst	ED conv.	PG conv.	LB	PY	MPIP	2-MP	Alk. pyrazine	Others
ZnO-ZSM-5	99.1	100.0	9.4	8.2	0.5	53.1	20.3	8.5
Zn-ZSM-5	96.2	99.9	12.1	11.4	7.9	44.5	15.2	8.9
ZnO + ZSM-5	97.8	96.5	16.6	14.7	9.3	27.1	21.6	10.7
H-ZSM-5	98.8	95.2	17.9	16.6	7.0	23.3	24.7	10.5
ZnO-FER	98.9	99.4	20.6	6.6	14.2	26.0	28.6	3.9
ZnO-Beta	99.5	99.3	30.7	7.6	14.6	31.3	8.4	7.3
ZnO	77.4	85.7	22.7	4.6	2.4	59.2	3.5	7.6

ED = ethylene diamine; PG = propylene glycol; LB = low boilers; PY = pyrazine; MPIP = methyl piperazine; 2-MP = 2-methyl pyrazine. Reaction conditions: atmospheric pressure, temperature = 400 °C; WHSV = 1 h^{-1}; TOS = 2 h; ED : PG : water = 1 : 1 : 5 mole ratio.

References

[1] E. Felder and D. Pitre, in: *Analytical Profiles of Drug Substances*, ed. K. Florey, vol. 12 (Academic Press, New York, 1983), p. 433.
[2] T. Shoji, T. Nakaishi and M. Mikata, Japanese Patent 08225543 A2, 3 September 1996, to Heisei.
[3] Koei Chemical Co., Japanese Patent 5343512 (1978).
[4] Korea Research Institute of Chemical Technology, Japanese Patent 0552829 (1993).
[5] Tokai Electro-Chemical Co., Japanese Patent 5550024 (1980).
[6] Koei Chemical Co., Japanese Patent 0948763 (1997).
[7] L. Forni and P. Pollesel, J. Catal. 130 (1991) 403.
[8] L. Forni and S. Nestori, Stud. Surf. Sci. Catal. 41 (1988) 291.
[9] G.T. Fedolyak, L.A. Krichevskii and A.D. Kagarlitskii, Izv. Akad. Nauk Kaz. SSR, Ser. Khim. 5 (1989) 50.
[10] T. Shoji, T. Nakaishi and M.Mikata, German Patent 19629258 A1, 6 February 1997.
[11] G.T. Fedolyak, A.D. Kagarlitskii, L.A. Krichevskii and A.V. Morozov, Izv. Akad. Nauk Resp. Kaz., Ser. Khim. 6 (1992) 31.
[12] S.J. Kulkarni, M. Subrahmanyam and A.V. Rama Rao, Indian J. Chem. 32A(1) (1993) 28.
[13] R. Anand and B.S. Rao, Catal. Commun. 3 (2002) 29.
[14] A.W. Chester and Y.F. Chu, US Patent 4,350,835 (1982).
[15] Y. Ono, Catal. Rev.—Sci. Eng. 34 (1992) 179.
[16] F. Roessner, A. Hagen, U. Mroczek, H.G. Karge and K.-H. Steinberg, Stud. Surf. Sci. Catal. 75 (1993) 1707.
[17] M.S. Scurrell, Appl. Catal. 32 (1987) 1.
[18] L. Froni, G. Stern and M. Gatti, Appl. Catal. 29 (1987) 161.
[19] R.J. Argauer and G.R. Landolt, US Patent 3,702,886 (1972).
[20] R.K. Ahedi and A.N. Kotasthane J. Porous Mat. 4 (1997) 171.
[21] V.L.J. Joly, P.A. Joy, S.K. Date and C.S. Gopinath, Phys. Rev. B 65 (2002) 184416/1-11
[22] J.J. Yeh and I. Lindau, At. Data Nucl. Data Tables 32 (1985) 1.
[23] E.P. Parry, J. Catal. 2 (1963) 371.
[24] R. Barthos, F. Lonyi, Gy. Onyestyak and J. Valyon, J. Phys. Chem. B 104 (2000) 7311.
[25] W.L. Earl, P.O. Fritz, A.A.V. Gibson and J.H. Lunsford, J. Phys. Chem. 91 (1987) 2091.
[26] K. Osaka, K.N. Nakashiro and Y. Ono, Bull. Chem. Soc. Jpn. 66 (1993) 755.
[27] F. Roessner, A. Hagen, U. Mroczek, H.G. Karge and K.H. Steinberg, Stud. Surf. Sci. Catal. 75B (1993) 1707.
[28] J.A. Biscardi and E. Iglesia, Catal. Today 31 (1996) 207.
[29] C.D. Wagner, W.M. Riggs, L.E. Davis, J.F. Moulder and G.F. Muilenberg, *Handbook of X-ray Photoelectron Spectroscopy* (Perkin-Elmer Corporation, Physical Electronics Division, Eden Prairie, MN, 1979), and references therein.